MICROSTRUCTURES AND PROPERTIES OF RAPID SOLIDIFICATION PROCESSED ALUMINUM-HIGH LITHIUM ALLOYS

P. Meschter, J.K. Gregory, R. Lederich, J. O'Neal, E. Lavernia, N. Grant

JOURNAL DE PHYSIQUE
Colloque C3, supplément au n°9, Tome 48, septembre 1987

MICROSTRUCTURES AND PROPERTIES OF RAPID SOLIDIFICATION PROCESSED ALUMINUM-HIGH LITHIUM ALLOYS

P.J. MESCHTER, J.K GREGORY, R.J. LEDERICH, J.E. O'NEAL, E.J. LAVERNIA* and N.J. GRANT*

McDonnell Douglas Research Laboratories, Saint-Louis, MO 63166, U.S.A.
**Department of Materials Science and Engineering, Massachusetts Institute of Technology, Cambridge, MA 02139, U.S.A.*

ABSTRACT

This paper reviews research at McDonnell Douglas Research Laboratories (MDRL) on alloy development, simplified processing, fatigue behavior, corrosion resistance, and superplastic forming of rapid solidification processed (RSP) Al-high Li alloys.

INTRODUCTION

RSP Al-Li alloys containing 4-5 wt% Li have significantly lower densities and higher elastic moduli than commercial 2XXX, 7XXX, and ingot-metallurgical (I/M) Al-Li alloys. For instance, an RSP Al-4Li-1Mg-0.2Zr extrusion is as strong as 7050-T76 (1), but has 14% lower density (2.41 g/cm^3) and 22% higher elastic modulus (86 GPa). Ductilities of Al-4Li alloys in peak-aged tempers are marginal (3-6%) as the result of intense planar slip resulting from high δ' concentrations and high concentrations of oxide inclusions traceable to the reactivity of the original melts and gas-atomized powders (1). Recent research on RSP Al-4Li alloys at MDRL has concentrated on compositional modifications and novel processing to improve ductility, fatigue and corrosion resistance, and superplastic formability.

ALLOY DEVELOPMENT

The composition Al-4Li-1Mg-0.2Zr was modified as shown in Table 1. Germanium was added to produce fine, insoluble particles which disperse planar slip (2), and silicon was expected to have a similar effect. Cerium was expected to getter the alloy melt and divert oxygen from Al-Li oxide inclusions. Lowering the Zr concentration to 0.03 wt% was intended to produce a recrystallized grain structure in which high-angle grain boundaries would act as slip barriers. Increasing the Zr concentration to 0.5 wt% promotes formation of α' [Al_3(Li,Zr)] "composite" precipitates, which are more resistant to dislocation shear than is δ' (3).

Ductilities of extrusions of the modified alloys, produced by conventional powder-metallurgical processing (Figure 1a), show small improvements relative to that of the baseline alloy except for Al-4Li-1Mg-0.5Ge-0.2Zr (Table 1). The ductility improvement in this alloy probably results from precipitation of fine, pure Ge particles during aging, as demonstrated by Cassada et al. (2). This alloy also contains AlLiGe, which diverts Li from δ' and lowers the yield stress. Detailed microstructural examination is required to determine the Ge concentration at which only the slip-dispersing particles are present. The Al-4Li-1Mg-0.03Zr alloy has slightly improved ductility at the expense of reduced Hall-Petch strengthening as a result of recrystallization, and the other alloys do not offer improvements in properties relative to those of the baseline alloy.

SIMPLIFIED PROCESSING

Conventional consolidation of RSP Al alloy powders (Figure 1a) is time- and labor-intensive. Atomized powders are exposed to oxygen-bearing atmospheres and form thin oxide skins, which appear as numerous fine oxide particles in the final products. These particles do not contribute to mechanical properties and may reduce ductility and toughness by promoting crack formation. Processes involving direct deposition of molten alloy droplets on a substrate to produce high-density preforms avoid these problems and have thus attracted attention recently. MDRL and the Massachusetts Institute of Technology (M.I.T.) have applied one such process, liquid-dynamic compaction (LDC), to the alloy Al-4Li-1Cu-0.2Zr with the objective of producing a clean product having a ductility and notch sensitivity superior to those of powder-processed Al-4Li alloys.

In LDC, partly molten, ultrasonically-atomized droplets impinge on a cooled substrate to produce a 98-99% dense compact which can be processed directly to extrusion or sheet (Figure 1b). Since atomized particles impinge immediately onto the compact, the free surface area and hence the oxygen concentration and inclusion density in the final product are substantially reduced. The cooling rate of aluminum alloys in LDC is ~ 10^3 K/s, compared to 10^4 - 10^5 K/s for ultrasonically atomized powders (4). This limitation does not significantly degrade the microstructures of those alloys that do not possess large concentrations of insoluble particles. Further details of LDC are given in reference (4).

Liquid-dynamic compacts of Al-4Li-1Cu-0.2Zr were processed into 0.20-cm (0.080-in.) thick sheets and a 1-cm (0.4-in.) diameter cylindrical extrusion. The conventional P/M extrusion (1) and the LDC extrusion have similar densities and compositions. The two types of extrusions have similar concentrations of δ (AlLi) and T_2 constituent particles (Figure 2), but the LDC extrusion is virtually free of the oxide particles which appear in profusion in the P/M extrusion. The oxygen concentration in the LDC extrusion is approximately 20 ppm compared with 600-1000 ppm in the conventional extrusion, in agreement with the observed microstructures.

The ductilities and notch tensile stress/yield stress ratios of LDC sheets in both longitudinal and transverse directions are superior to those of sheets rolled from the P/M extrusion (Table 2). Microstructural examination and texture analyses of the sheets show that the lower yield stresses of the LDC sheets are associated with weaker textures and larger subgrain diameters which result from the smaller degree of warm working required to produce the LDC sheets. The LDC extrusion has a strong fiber texture and hence a higher longitudinal strength than the P/M extrusion, while retaining superior notch sensitivity owing to its low oxygen concentration. The fracture surface of a notched LDC extrusion specimen shows a torturous fracture surface indicative of high energy absorption (Figure 3b), while the P/M extrusion has a much flatter fracture surface indicative of high notch sensitivity (Figure 3a).

FATIGUE BEHAVIOR

The fatigue behavior of longitudinal (L) and transverse (T) specimens of peak-aged Al-4Li-0.2Zr extrusions (1) was examined. Part of the aging treatment was done after machining to help relieve residual stresses, and approximately 500 µm was removed from the diameter of each specimen by electropolishing prior to testing. Figure 4 shows the S-N curves for L and T specimens. Crack initiation in L specimens always occurred at foreign particles. At longer lifetimes, there is a greater tendency for internal crack nucleation. A transition from external to internal nucleation as fatigue life increases has been found at ~ 10^7 cycles for several materials (5-7). Numerous large (50 µm) particles in extruded Al-4Li-0.2Zr evidently cause the transition to occur at 3 x 10^4 cycles. Three distinct types of cracks were observed: a "plane" crack (Figure 5a); a "chisel" crack (Figure 5b); and a "cone" crack (Figure 5c). No correlation was found between initiation site type and crack type. All of the L-samples showed angles of 27-37° between the fatigue crack and the stress axis.

The paucity of data for T-samples is due to a tendency for these specimens to fail in the threads. Apparently, this material is extremely notch sensitive in the transverse direction. An example of failure in a T-specimen is given in Figure 5d. No foreign particle was found at the nucleation site. Propagation of these cracks was always in the short transverse direction.

Analyses of (111), (200), and (220) pole figures obtained by neutron diffraction showed a predominant (110)<112> preferred orientation. For both L and T specimens, fracture surfaces apparently coincide with {111} planes. For L specimens, these {111} planes have Schmid factors of 0.41 and thus experience the maximum resolved shear stress. For T-specimens, the maximum Schmid factor for any {111} plane is 0.27; however, crack growth occurs on a set of {111} planes for which the Schmid factor is zero. In this case, crack propagation is controlled by tensile rather than shear stresses. This behavior has been observed for Stage I fatigue cracks in a nickel base superalloy (8). These cracks propagate on {111} planes in <110> directions, as did cracks in T-samples of Al-4Li-0.2Zr. The analogy between these two materials is appropriate, since both consist of an fcc matrix with a precipitated $L1_2$ phase. Additional evidence of the influence of the $L1_2$ phase on fatigue behavior is provided by the extreme macroscopic deviations from Mode I cracking in L-direction specimens. These deviations, which are not normally found for aluminum alloys tested in air, are probably the result of strong slip planarity.

CORROSION RESISTANCE

Corrosion resistances in 3.5% aqueous NaCl solution of Al-high Li alloys containing Cu or Mg additions have been investigated. It has been shown (9) that Li additions to Al are not detrimental to corrosion behavior unless more than 10 vol% of the reactive phase δ (AlLi) is present. Otherwise, the corrosion resistance of Al-high Li alloys is equal or superior to that of 7XXX alloys in corrosion-resistant tempers. Corrosion rates were measured in 100-h weight-loss tests. The free corrosion potential, E_{corr}, was measured after 72 h. Values of E_{corr} and the corrosion current I_{corr} were obtained for both nitrogen-deaerated and non-deaerated solutions. Further details of the corrosion tests are in reference (9).

Table 3 shows the results of the various tests for alloys heat treated to optimize strength and ductility. Additions of Mg have little effect on corrosion behavior, but weight loss rates increase dramatically when Cu is added. This is probably related to the relatively noble values of E_{corr} measured in non-deaerated solutions. Values of the breakdown potential were approximately -0.78 to -0.82 V, independent of alloy, heat treatment, or deaeration. The only exceptions were the Cu-containing alloys in the non-deaerated solution, for which no breakdown potential could be measured. In this case, E_{corr} is at or above the breakdown potential, and the passivation region is effectively eliminated.

SUPERPLASTIC FORMING

Net-shape processing techniques such as superplastic forming minimize usage of expensive materials and hence are particularly important to RSP Al-4Li alloys. The conditions of strain rate and temperature under which RSP Al-4Li-0.2Zr can be superplastically formed have been determined at MDRL in biaxial (cone-forming) tests (10). Incremental-strain-rate (ISR) and constant-strain-rate (CSR) tests were conducted on 0.225- to 0.245-cm-thick sheets at 590°C under a superimposed hydrostatic pressure of 2.1 to 2.8 MPa to suppress cavitation.

Results of ISR experiments (Table 4) show that RSP Al-4Li-0.2Zr is formable to large superplastic strains, while CSR tests yielded modest strains. The strain-rate-sensitivity exponent m is 0.33-0.36, typical of Zr-containing Al-Li alloys which have fully-recovered substructures prior to thermomechanical processing of superplastically formable sheets. Following a suggestion by Ghosh (11), two experiments were conducted at a high strain rate up to $\varepsilon_t = 0.5$, followed by relaxation to a lower rate for the remainder of the test. This procedure promoted the continuous formation of favorably-oriented high-angle boundaries early in the test, and thus resulted in an improvement in strain to failure relative to that of experiments conducted entirely at lower strain rates.

RSP Al-4Li-0.2Zr undergoes flow-softening during CSR tests (Figure 6). Examination of microstructural development during forming (11) shows that flow-softening is the result of continuous formation of more nearly equiaxed grains during testing. The effectiveness of the initial high strain rate in producing a favorable microstructure for subsequent forming (experiment 6) is borne out by the lower flow stress in the latter (low-strain-rate) portion of this experiment relative to that of experiment 4, which was conducted at the lower strain rate throughout. Since cavitation was completely suppressed in these tests, density measurements of various sections of the cone were used to evaluate Li loss by evaporation or oxidation during forming. The maximum decrease in Li concentration was from 4.0 to 3.8 wt%, and it is concluded that lithium loss should not degrade the post-formed mechanical properties of Al-4Li alloy parts superplastically formed at or above a strain rate of 6×10^{-4} s^{-1}.

CONCLUSIONS

1. Modest improvements in ductility can be achieved in RSP Al-4Li alloys by additions of Ge, which forms fine, slip-dispersing dispersoids during heat treatment.

2. Simplified processing by liquid-dynamic compaction improves the ductility and notch sensitivity of Al-4Li-1Cu-0.2Zr extrusions and sheet by reducing the volume fractions of oxide dispersoids and inclusions.

3. A transition from external to internal crack nucleation is found for L-specimens of peak-aged Al-4Li-0.2Zr as fatigue life increases. This transition occurs at relatively short lifetimes owing to the high concentration of foreign particles.

4. Fatigue behavior is anisotropic in extruded Al-4Li-0.2Zr. Stage I crack propagation is controlled by shear stresses in L-specimens, and by tensile stresses in T-specimens.

5. Additions of Mg to Al-high Li alloys do not significantly affect corrosion behavior. Additions of Cu degrade corrosion resistance by raising the free corrosion potential to the value of the breakdown potential and eliminating the passivation region.

6. Al-4Li-0.2Zr is superplastically formable at 590°C without excessive lithium losses. Optimal SPF conditions involve initial high forming rates to continuously produce favorably oriented high-angle boundaries. Application of a suitable hydrostatic pressure completely suppresses cavitation.

ACKNOWLEDGEMENT

This research was conducted under the McDonnell Douglas Corp. Independent Research and Development program.

REFERENCES

1. P. J. Meschter, R. J. Lederich, and J. E. O'Neal, in Aluminum-Lithium Alloys III, C. Baker, P. J. Gregson, S. J. Harris, and C. J. Peel, eds., The Institute of Metals, London, 1986, pp. 85-96.
2. W. A. Cassada, G. J. Shiflet, and E. A. Starke, Jr., Acta Metall. 34, 367-378 (1986).

3. F. W. Gayle, J. B. VanderSande, and O. R. Singleton, in Aluminum Alloys: Their Physical and Mechanical Properties, E. A. Starke, Jr., and T. H. Sanders, Jr., eds., Engineering Materials Advisory Services, Ltd., Warley, England, 1986, pp. 767-781.
4. E. J. Lavernia, G. Rai, and N. J. Grant, Int. J. Powd. Met. 22, 9-16 (1986).
5. G. C. George, in Corrosion Fatigue: Chemistry, Mechanics, and Microstructure, O. Devereux and A. J. McEvily, eds., National Association of Corrosion Engineers, Houston, 1972, pp. 459-467.
6. D. F. Neal and P. A. Blenkinsop, Acta Metall. 24, 59-63 (1976).
7. J. M. Hyzak and I. M. Bernstein, Metall. Trans. 13A, 33-44 (1982).
8. M. Gell and G. R. Leverant, Acta Metall. 16, 553-561 (1968).
9. J. K. Gregory, P. J. Meschter, and J. E. O'Neal, in reference (3), pp. 1227-1235.
10. P. J. Meschter, R. J. Lederich, and S. M. L. Sastry, Metall. Trans. 18A (in press).
11. A. K. Ghosh and C. Gandhi, in Strength of Metals and Alloys, Proceedings of the 7th International Conference, H. J. McQueen, J.-P. Bailon, J. I. Dickson, J. J. Jonas, and M. G. Akben, eds., Pergamon Press, Oxford, England, 1985, pp. 2065-72.

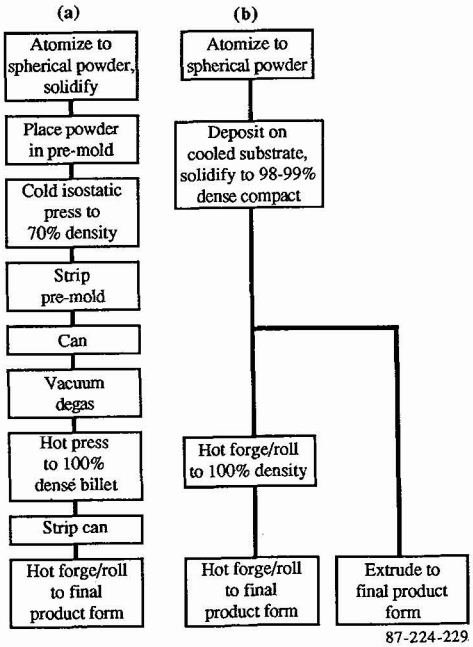

Figure 1. Consolidation sequences for Al alloy powders: (a) conventional and (b) liquid-dynamic compaction.

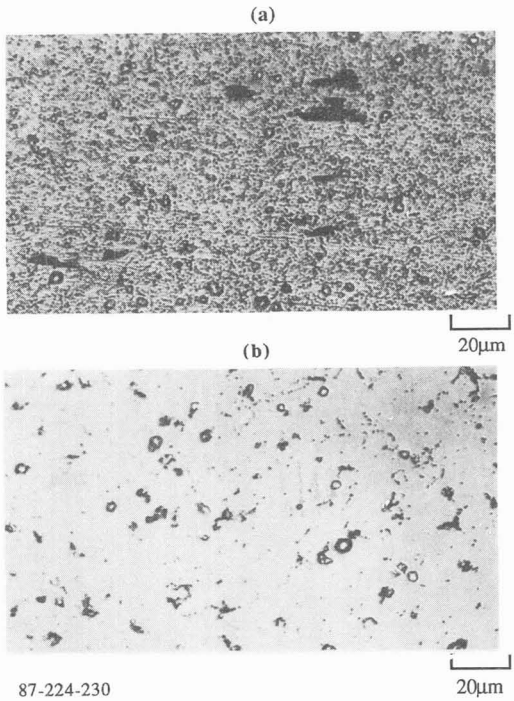

Figure 2. Microstructures of RSP Al-4Li-1Cu-0.2Zr extrusions: (a) from gas-atomized powder and (b) from a liquid-dynamic compact. Solution-treated 560°C/1h.

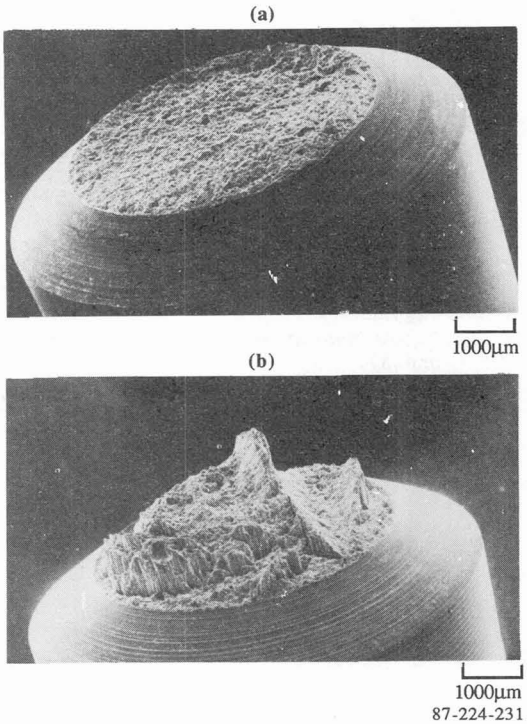

Figure 3. Notched-specimen fracture surfaces of peak-aged Al-4Li-1Cu-0.2Zr extrusions: (a) from gas-atomized powder and (b) from a liquid-dynamic compact.

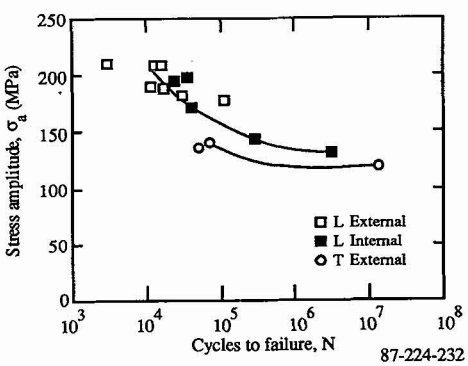

Figure 4. S-N fatigue behavior of Al-4Li-0.2Zr, solution-treated 588°C/1h and aged 160°C/48h. Specimens tested in air at 30 Hz and R = 0.1.

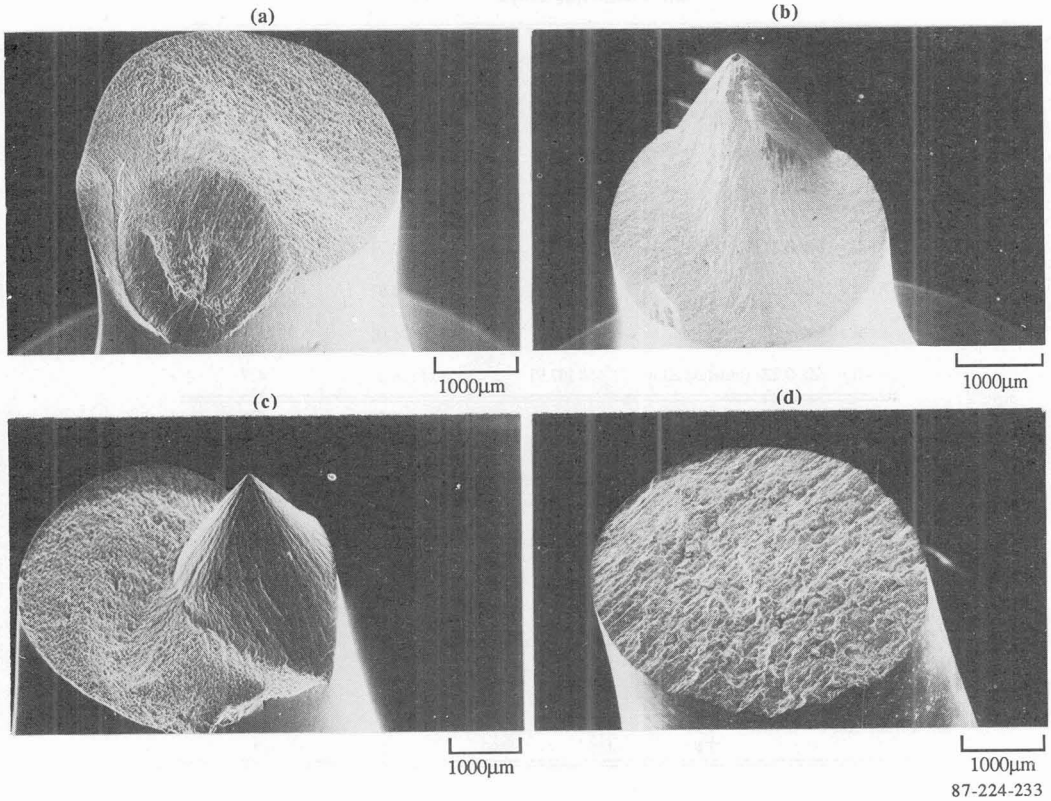

Figure 5. Fracture surfaces of peak-aged Al-4Li-0.2Zr fatigue specimens: (a) L-specimen, "plane" crack, (b) L-specimen, "chisel" crack, (c) L-specimen, "cone" crack, and (d) T-specimen (arrow indicates crack origin).

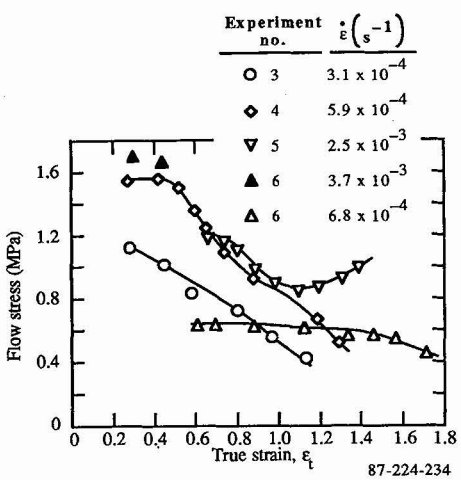

Figure 6. Flow stress as a function of forming strain during superplastic forming of RSP Al-4Li-0.2Zr at 590°C.

Table 1. Mechanical properties of peak-aged, modified RSP Al-4Li-1Mg alloys.

Alloy composition	Yield stress (MPa [ksi])	Ultimate tensile stress (MPa [ksi])	Elongation (%)
Al-4Li-1Mg-0.6Si-0.2Zr	440 [63.7]	472 [68.5]	3.6
Al-4Li-1Mg-0.2Ge-0.2Zr	429 [62.2]	471 [68.3]	5.5
Al-4Li-1Mg-0.5Ge-0.2Zr	430 [62.3]	487 [70.6]	6.4
Al-4Li-1Mg-0.5Ce-0.2Zr	450 [65.3]	502 [72.7]	4.7
Al-4Li-1Mg-0.03Zr	417 [60.4]	516 [74.8]	5.6
Al-4Li-1Mg-0.5Zr	470 [68.2]	510 [74.0]	5.1
Al-4Li-1Mg-0.2Zr (baseline alloy)	468 [67.9]	524 [76.0]	4.9

87-224-235

Table 2. Smooth and notched-specimen mechanical properties of various RSP Al-4Li-1Cu-0.2Zr product forms.

Product form	Temper	Yield stress (YS) (MPa)	Ultimate tensile stress (MPa)	Elongation (%)	Notch tensile stress (NTS) (MPa)	NTS/YS ratio
P/M extrusion	T6	473	510	3.8	195	0.41
Extrusion from LDC	T6	503	568	4.2	440	0.87
Sheet from P/M extrusion	T6	470	502	2.1	144	0.31
	T8	506	529	1.6	93	0.18
Sheet from LDC	T6	391	476	5.0	200	0.51
	T8	420	499	5.1	267	0.64

87-224-236

Table 3. Biaxial superplastic forming experiments on rapid solidification processed Al-4Li-0.2Zr at 590°C.

Experiment no.	Strain rate, $\dot{\varepsilon}$ (s^{-1})	True strain at failure, ε_t	Engineering strain at failure, ε (%)	Strain-rate sensitivity exponent, m
1	2.3×10^{-5} – 3.1×10^{-3} (incremental)	2.40	1000	0.36
2	1.0×10^{-4} – 3.5×10^{-3} (incremental)	1.92	590	0.33
3	3.1×10^{-4}	1.24	250	–
4	5.9×10^{-4}	1.35	290	–
5	2.5×10^{-3}	1.53	360	–
6	3.7×10^{-3} to $\varepsilon_t = 0.5$, then 6.8×10^{-4}	1.79	500	–
7	4×10^{-3} to $\varepsilon_t = 0.5$, then 7×10^{-4} (not instrumented)	>2.2	>800	–

87-224-238

Table 4. Corrosion rates and potentiodynamic data for the alloys investigated.

Alloy	Corrosion rate (mm/yr)	Deaerated		Not deaerated	
		E_{corr} (V vs SCE)	I_{corr} ($\mu A/cm^2$)	E_{corr} (V vs SCE)	I_{corr} ($\mu A/cm^2$)
Al-3Li*	0.027	–1.48	2.1	–1.11	0.1
Al-3Li-0.2Zr*	<0.01	----	----	–1.32	0.3
Al-3Li-1Mg-0.2Zr	----	–1.50	2.5	–1.11	0.05
Al-3Li-2Mg-0.2Zr	----	–1.10	1.6	–1.36	0.2
Al-3Li-1Cu-0.2Zr	0.018	–1.29	1.3	–0.79	0.7
Al-4Li-0.2Zr*	<0.01	–1.47	4.6	–1.06	0.3
Al-4Li-1Mg-0.2Zr	<0.01	–1.22	0.4	–1.13	13.5
Al-4Li-2Mg-0.2Zr	0.08	–1.13	0.8	–1.05	0.4
Al-4Li-1Cu-0.2Zr	0.055	–1.28	3.2	–0.79	1.0
Al-4Li-2Cu-0.2Zr	0.43	----	----	----	----
Al-5Li-0.2Zr*	0.020	–1.55	5.1	–1.00	0.03
Al-5Li-1Mg-0.2Zr	0.065	–1.09	10.7	–1.03	0.4
Al-5Li-2Mg-0.2Zr	0.019	–0.96	0.08	–1.06	0.1
Al-5Li-1Cu-0.2Zr	0.28	–1.26	4.5	–1.15	1.9
Al-5Li-2Cu-0.2Zr	0.45	–1.21	4.3	–0.86	1.5

* – Solution heat treated at 588°C, aged 48 hours at 160°C. All other alloys solution heat treated at 560°C, aged 48 hours at 160°C.

87-224-237